

Micro concrete model tests with heavy projectiles dropped from low heights

S.Wicks, D.Barnes & G.Garton

Atomic Energy Establishment, Winfrith, Dorset, UK

1. INTRODUCTION

Reactors can be subjected to several forms of impact. An example of a high mass low velocity impact would be a dropped charge machine.

Formulae have been developed to calculate perforation velocities of targets hit by solid projectiles with low mass and at high velocity. The programme of work described below, seeks to establish the validity of these formulae when applied to heavy dropped objects. The work is being carried out at UKAEA Winfrith in parallel with tests on large scale models being undertaken by the CEGB at Cheddar England.

The parameters varied were concrete strength, reinforcement content, reinforcement bar frequency, span of target, single face and both face reinforcement, projectile mass, and projectile diameter.

The models tested were made of micro concrete reinforced with high strength drawn wire.

2 TARGETS

The targets were all 767 mm square, 83 mm thick and made of microconcrete reinforced with high strength drawn wire. All the models had reinforcement that was the same in each direction, but the bar diameters and frequencies were varied. Some models had reinforcement at both faces and the remainder had reinforcement at only the surface remote from the impact. The cover to the inner bars was 8.5 mm. 2.5 mm and 4.0 mm drawn wire was used for the models, having 0.1% proof stresses of 726 MPa and 484 MPa, ultimate stresses of 763 MPa and 500 MPa, and elastic moduli of 193 GPa and 197 GPa respectively. The concrete compressive strengths were taken as the average of nine 300 mm high by 150 mm diameter cylinders, and ranged from 32.7 to 51.2 MPa.

3 TEST PROCEDURE

Figure 1 shows the test arrangement. The targets were bedded onto concrete supports along each of their four sides so that there was a clear span of either 415 or 630 mm. A high speed camera recording 3000 frames each second was set up opposite a graduated scale so that the missile velocity before and after impact could be observed. Four different projectiles were used, as listed in Table 1. The projectile

was raised to the height necessary to obtain the required velocity and supported by a fuse wire release mechanism. Time delays in the firing sequence allowed the camera to reach its correct running speed by the time that the impact occurred.

4 DISCUSSION OF RESULTS

Table 1 lists the perforation velocities measured during the tests as "Actual Perforation Velocity". Figure 2 shows the correlation between the measured perforation velocities and perforation velocities predicted by equation 1. This equation was based on the CEA/EDF formula, Berriaud (1978), but modified for reinforcement and concrete compressive strength. The reinforcement factor was suggested by Barr (1983) and 37 MPa was used as the maximum value for the concrete compressive strength as suggested by Gittus (1982). The perforation velocity is then

$$Vc1 = 1.3 \sigma^{1/2} \rho^{1/6} \left(\frac{e^2 d}{M}\right)^{2/3} (r + 0.3)^{1/2} \quad (1)$$

These values of perforation are listed as column Vc1 in Table 1. If instead of applying a limit of 37 MPa to the concrete strength it is assumed that the strengths of all models is 37 MPa there appears to be no loss of accuracy. This suggests that the perforation velocity of a concrete target is not sensitive to the concrete strength for the range of strength used, as shown in Figure 3. Column Vc2 lists the predicted velocities assuming that the compressive strength of all the models was 37 MPa.

$$Vc2 = 1.3 (37 \times 10^6)^{1/2} \rho^{1/6} \left(\frac{e^2 d}{M}\right)^{2/3} (r+0.3)^{1/2} \quad (2)$$

To improve the correlation between the predicted and actual perforation velocities, equation 2 has been multiplied by factors relating to the different parameters used. These non-dimensional terms have been chosen by observing the effects of changing the parameters within the models and raising the term to a suitable power. There is no fundamental basis for these terms. The presence of reinforcement at only one surface of a target reduced the perforation velocity compared to that of a target reinforced at both faces but this effect was small. Nevertheless, to reduce the error between the predicted and measured perforation velocities, equation (2) was modified to become equation (3). Where there was no impact face reinforcement, the term K in equation (3) was set to 1 and when reinforcement was present at both faces K was set to 0. Figure 4 shows the comparison between the measured perforation velocity and the velocity predicted by the equation

$$Vc3 = 1.3 (37 \times 10^6)^{1/2} \rho^{1/6} \left(\frac{e^2 d}{M}\right)^{2/3} \left((1-K \left(\frac{0.005d}{s}\right)^{1/2}) r + 0.3 \right)^{1/2} \quad (3)$$

Column Vc3 of Table 1 lists these predicted values.

The tests suggested that where the reinforcement was spaced more closely for the same reinforcement content, a greater energy was needed for perforation with the concrete breaking into many more smaller pieces compared to models with reinforcement at larger spacing. The perforation velocity was therefore modified to

$$Vc4 = Vc3 \left(\frac{e}{2.5 s} \right)^{1/6} \quad (4)$$

This produced the predictions shown as Vc4 in Table 1 and plotted as Figure 5.

The comparison between the measured and predicted perforation velocities was further improved by incorporating the effect of span, because as the span was reduced the perforation velocity also reduced. This perforation velocity was then

$$Vc5 = Vc4 \left(\frac{l}{6.8e} \right)^{1/2} \quad (5)$$

The values of Vc5 are shown in Table 1 and plotted as Figure 6.

The incorporation of the effect of reinforcement was based on its area, without taking into account the strengths which varied by a large amount as listed in section 2. This suggests that the reinforcement contributed to the impact resistance of the models through its stiffness or elastic modulus and not through its strength.

5 CONCLUSIONS

Variation of the concrete strength of the models tested did not appear to affect the perforation velocity.

The impact surface reinforcement did not contribute very much towards the perforation velocity.

Models with similar areas of reinforcement at different spacing had different perforation velocities. The models with closer reinforcement had the higher perforation velocity.

Models with greater spans possessed higher perforation velocities.

The perforation velocity was not affected by the reinforcement strength.

6 NOMENCLATURE

d	projectile diameter	r	reinforcement percentage
e	concrete thickness	s	reinforcement spacing
K	constant (1 or 0)	ρ	concrete density
l	model clear span	σ	concrete compressive cylinder strength
M	projectile mass		

REFERENCES

- Berriaud, C., Sokolovsky, A., Gueraud, R., Dulac, J., Labrot, R. Local Behaviour of Reinforced Concrete Walls Under Missile Impact. Nuclear Engineering and Design, (1978) 457-469, North Holland Publishing Company.
- Barr, P., Carter, P.G., Howe, W.D., Neilson, A.J., Richards, A.E. Experimental Studies of the Impact Resistance of Steel Faced Concrete Composites. 7th Conference of Structural Mechanics in Reactor Technology, Chicago, USA, August 22-26, 1983, Paper J8/4.
- Gittus, J.H. PWR Degraded Core Analysis. UKAEA Northern Division Report ND- R-610(S), April 1982, H M Stationery Office, (pages 386-387).

Table 1. Model dimensions and perforation velocities

Model No.	Reinf. dia. mm	Reinf. s mm	α MPa	M kg	d mm	l mm	Actual					
							Perf. vel. m/sec	Vc1 m/s	Vc2 m/s	Vc3 m/s	Vc4 m/s	Vc5 m/s
12	2.5 *	32.0	43.1	150.0	89	630	5.0	5.15	5.15	5.15	5.18	5.48
13	2.5 *	32.0	42.6	159.4	150	630	6.8	7.01	7.01	7.01	7.05	7.45
14	2.5 *	10.0	33.4	150.0	89	630	>7.7	6.63	6.98	6.98	8.53	9.01
15	2.5	10.0	32.	150.0	89	630	>7.7	6.56	6.98	6.48	7.91	8.36
17	2.5	32.0	36.6	150.0	89	630	5.7	5.12	5.15	5.03	5.07	5.35
21	2.5 *	15.0	33.1	150.0	89	630	>7.7	5.83	6.16	6.16	7.03	7.43
22	2.5	15.0	30.5	150.0	89	630	7.1	5.59	6.16	5.85	6.68	7.06
23	4.0 *	40.5	38.7	150.0	89	630	7.7	6.07	6.07	6.07	5.87	6.21
24	4.0	40.5	37.2	150.0	89	630	6.0	6.07	6.07	5.89	5.70	6.02
25	2.5 *	21.0	39.0	150.0	89	630	>7.7	5.64	5.64	5.64	6.09	6.43
26	2.5	21.0	33.7	150.0	89	630	7.2	5.39	5.64	5.44	5.87	6.20
28	2.5 *	15.0	40.5	310.0	89	630	4.7	3.80	3.80	3.80	4.34	4.58
29	2.5 *	10.0	38.4	310.0	89	630	5.0	4.30	4.30	4.30	5.26	5.55
31	4.0	40.5	39.7	66.5	83	415	8.0	9.97	9.97	9.69	9.37	8.03
32	4.0	40.5	42.0	66.5	83	415	7.3	9.97	9.97	9.69	9.37	8.03
33	2.5	32.0	51.2	66.5	83	415	6.8	8.46	8.46	8.27	8.32	7.14
34	4.0	40.5	43.0	310.0	89	630	4.0	3.74	3.74	3.63	3.51	3.71
35	4.0 *	40.5	40.3	310.0	89	630	3.7	3.74	3.74	3.74	3.62	3.83
36	4.0 *	40.5	39.8	310.0	89	630	3.5	3.74	3.74	3.74	3.62	3.83
37	4.0 *	27.0	40.6	310.0	89	630	4.3	4.23	4.23	4.23	4.38	4.63
38	4.0 *	27.0	40.2	310.0	89	630	4.6	4.23	4.23	4.23	4.38	4.63
39	4.0 *	40.5	37.5	310.0	89	415	3.4	3.74	3.74	3.74	3.62	3.10
42	2.5 *	15.0	38.2	310.0	89	415	3.6	3.80	3.80	3.80	4.34	3.72
43	2.5 *	10.0	36.5	310.0	89	415	4.8	4.27	4.30	4.30	5.26	4.51
44	4.0	40.5	36.8	310.0	89	415	3.1	3.73	3.74	3.63	3.51	3.01
45	2.5	15.0	39.5	310.0	89	630	3.8	3.79	3.79	3.61	4.12	4.35
46	4.0	27.0	33.8	310.0	89	630	3.9	4.04	4.23	4.05	4.19	4.43
47	4.0	40.5	39.7	310.0	89	415	3.2	3.74	3.74	3.63	3.51	3.01
48	2.5	15.0	37.8	310.0	89	415	3.6	3.80	3.80	3.61	4.12	3.53
49	4.0 *	27.0	40.4	310.0	89	415	4.7	4.23	4.23	4.23	4.38	3.75
50	2.5	10.0	36.4	310.0	89	630	4.0	4.27	4.30	3.99	4.87	5.15
51	2.5	10.0	38.0	310.0	89	415	4.1	4.30	4.30	3.99	4.87	4.18
52	4.0	27.0	37.6	310.0	89	415	3.8	4.23	4.23	4.05	4.19	3.59

* Reinforcement in both directions at each face.

> 7.7 Maximum velocity possible, target not perforated.

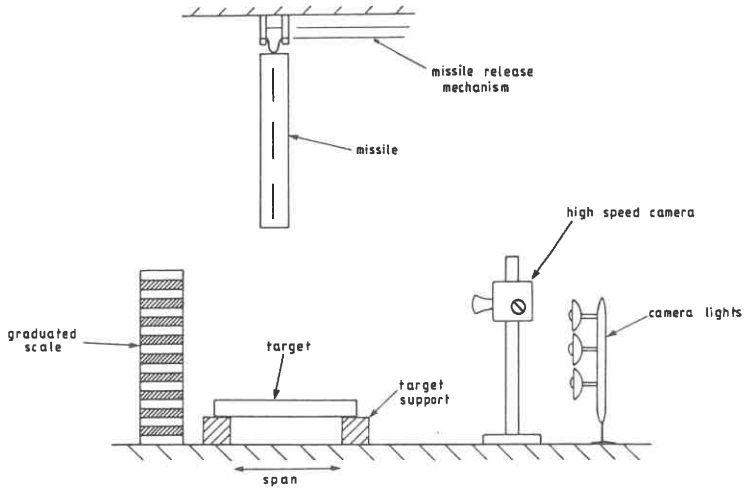


fig.1 Test arrangement

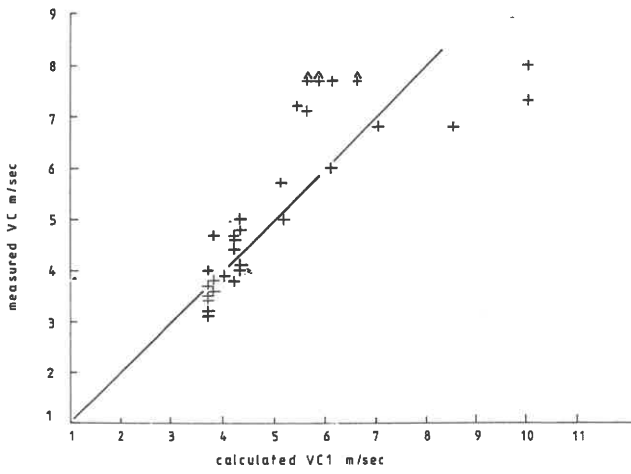


fig 2 Perforation velocities VC vs VC1

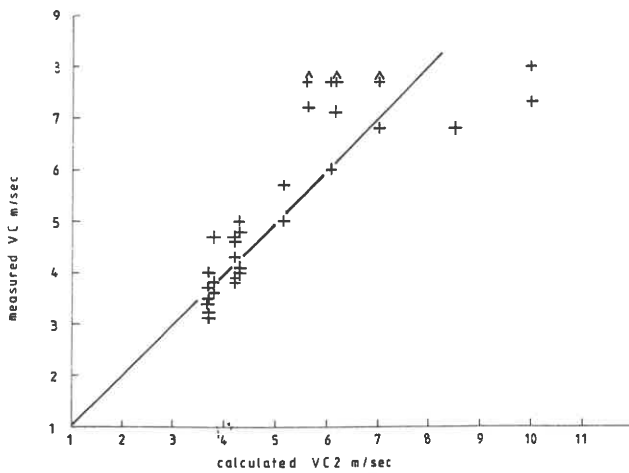


fig. 3 Perforation velocities VC vs VC2

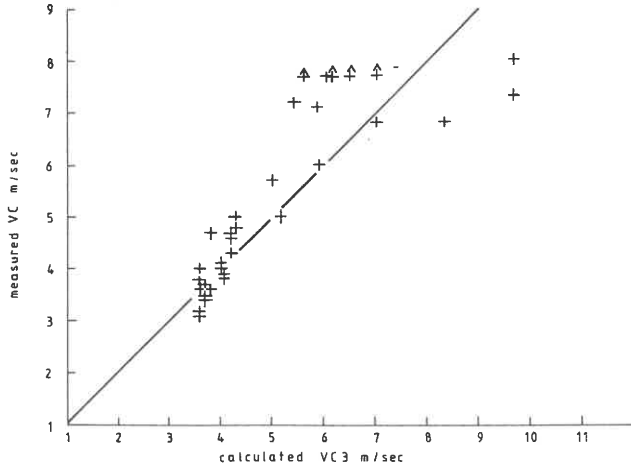


fig.4 Perforation velocities VC vs VC3

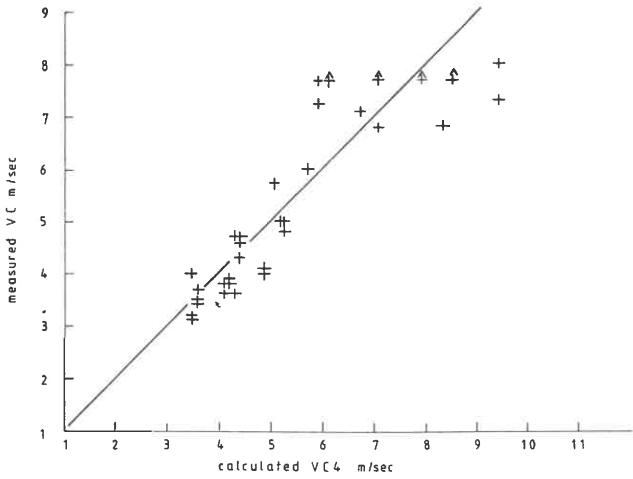


fig.5 Perforation velocities VC vs VC4

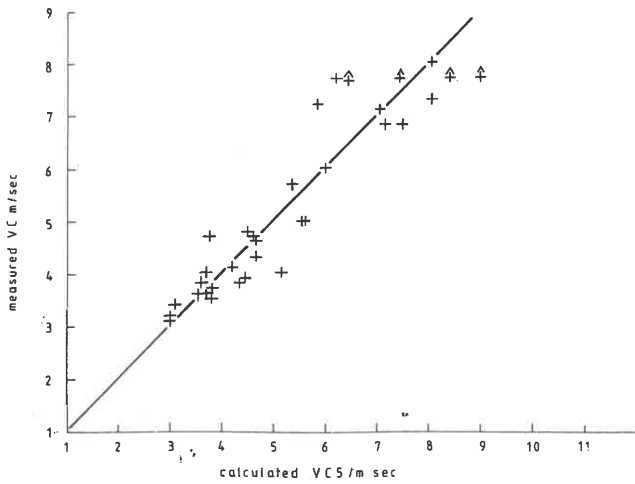


fig.6 Perforation velocities VC vs VC5